



**HAL**  
open science

## **A combined LC-MS and NMR approach to reveal metabolic changes in the hemolymph of honeybees infected by the gut parasite *Nosema ceranae***

Cyril C. Jousse, Céline Dalle, Angélique Abila, Mounir Traïkia, Marie Diogon, Bernard Lyan, Hicham El Alaoui, Cyril Vidau, Frédéric Delbac

### ► To cite this version:

Cyril C. Jousse, Céline Dalle, Angélique Abila, Mounir Traïkia, Marie Diogon, et al.. A combined LC-MS and NMR approach to reveal metabolic changes in the hemolymph of honeybees infected by the gut parasite *Nosema ceranae*. *Journal of Invertebrate Pathology*, 2020, 176, pp.107478. 10.1016/j.jip.2020.107478 . hal-03132817

**HAL Id: hal-03132817**

**<https://hal.uca.fr/hal-03132817>**

Submitted on 17 Oct 2022

**HAL** is a multi-disciplinary open access archive for the deposit and dissemination of scientific research documents, whether they are published or not. The documents may come from teaching and research institutions in France or abroad, or from public or private research centers.

L'archive ouverte pluridisciplinaire **HAL**, est destinée au dépôt et à la diffusion de documents scientifiques de niveau recherche, publiés ou non, émanant des établissements d'enseignement et de recherche français ou étrangers, des laboratoires publics ou privés.



Distributed under a Creative Commons Attribution - NonCommercial | 4.0 International License

1 **Title**

2 A combined LC-MS and NMR approach to reveal metabolic changes in the hemolymph of  
3 honeybees infected by the gut parasite *Nosema ceranae*

4 Authors : Cyril Jousse<sup>2,3\*</sup>, Céline Dalle<sup>2,3</sup>, Angélique Abila<sup>2,3</sup>, Mounir Traikia<sup>2,3</sup>, Marie Diogon<sup>1</sup>,  
5 Bernard Lyan<sup>2,3</sup>, Hicham El Alaoui<sup>1</sup>, Cyril Vidau<sup>4</sup>, Frédéric Delbac<sup>1</sup>

6

7 <sup>1</sup> Université Clermont Auvergne, CNRS, Laboratoire "Microorganismes : Génome et  
8 Environnement", F-63000 Clermont–Ferrand, France.

9 <sup>2</sup> Université Clermont Auvergne, CNRS, Sigma-Clermont, Institut de Chimie de Clermont-  
10 Ferrand, F-63000, Clermont-Ferrand, France.

11 <sup>3</sup> Plateforme d'Exploration du Métabolisme, Université Clermont Auvergne & I.N.R.A site de  
12 Theix, Clermont-Ferrand, France.

13 <sup>4</sup> ITSAP, UMT PrADE, Inra – Acta, 228 route de l'aérodrome, F-84000, Avignon, France  
14 (current address).

15

16 \* Corresponding author.

17 Email: [cyril.jousse@uca.fr](mailto:cyril.jousse@uca.fr); Address: Institute of Chemistry of Clermont-Ferrand, 24 avenue  
18 Blaise Pascal, 63178 Aubière cedex, France

19

20 **Highlights**

21 \* Honeybee hemolymph metabolome is altered by the gut parasite *Nosema ceranae*

22 \* 15 metabolites were identified by LC-MS and NMR as candidate biomarkers of infection

23 \* Putative biomarkers are involved in carbohydrate, amino acid and lipid metabolic  
24 pathways

25

26 **Abstract**

27 *Nosema ceranae* is an emerging and invasive gut pathogen in *Apis mellifera* and is  
28 considered as a factor contributing to the decline of honeybee populations. Here, we used a  
29 combined LC-MS and NMR approach to reveal the metabolomics changes in the hemolymph  
30 of honeybees infected by this obligate intracellular parasite. For metabolic profiling,  
31 hemolymph samples were collected from both uninfected and *N. ceranae*-infected bees at  
32 two time points, 2 days and 10 days after the experimental infection of emergent bees.  
33 Hemolymph samples were individually analyzed by LC-MS, whereas each NMR spectrum was  
34 obtained from a pool of three hemolymphs. Multivariate statistical PLS-DA models clearly  
35 showed that the age of bees was the parameter with the strongest effect on the metabolite  
36 profiles. Interestingly, a total of 15 biomarkers were accurately identified and were assigned  
37 as candidate biomarkers representative of infection alone or combined effect of age and  
38 infection. These biomarkers included carbohydrates ( $\alpha/\beta$  glucose,  $\alpha/\beta$  fructose and  
39 hexosamine), amino acids (histidine and proline), dipeptides (Glu-Thr, Cys-Cys and  $\gamma$ -Glu-  
40 Leu/Ile), metabolites involved in lipid metabolism (choline, glycerophosphocholine and O-  
41 phosphorylethanolamine) and a polyamine compound (spermidine). Our study  
42 demonstrated that this untargeted metabolomics-based approach may be useful for a better  
43 understanding of pathophysiological mechanisms of the honeybee infection by *N. ceranae*.

44 **Keywords:** Honeybee; Metabolomic; *Nosema ceranae*; Stress Biomarkers

45

46

47 **1. Introduction**

48 Honeybees provide essential ecosystem services in agricultural and natural areas by  
49 pollinating many crops and native plants. However, these insect pollinators are exposed to  
50 multiple abiotic (pollutants, pesticides) and biotic (infectious agents, parasites) stressors  
51 which are detrimental to their health and lifespan. Among them, both parasites and  
52 pesticides seem to be the most important stressors affecting honeybees and contribute to  
53 the decline of their populations (Goulson et al., 2015; vanEngelsdorp et al., 2009;  
54 vanEngelsdorp and Meixner, 2010).

55

56 The gut parasite *Nosema ceranae* is among the most common pathogens in *Apis mellifera*,  
57 with a worldwide distribution (Goulson et al., 2015) and is now considered to be a major  
58 threat to the Western honeybee at both the individual and colony levels (Fries, 2010; Higes  
59 et al., 2013; Paris et al., 2018; vanEngelsdorp and Meixner, 2010). Similar to other  
60 microsporidian species, *N. ceranae* can alter the bee physiology and behavior in order to  
61 maintain a more favorable environment for its reproduction. Several studies have  
62 demonstrated that *N. ceranae* infection impairs tissue integrity in the midgut (Dussaubat et  
63 al., 2012), alters the energy demand in honey bees (Alaux et al., 2009; Martín-Hernández et  
64 al., 2011; Mayack and Naug, 2009; Naug and Gibbs, 2009) and decreases hemolymph sugar  
65 level (Mayack and Naug, 2010). The infection also significantly suppresses the bee immune  
66 response (Alaux et al., 2009; Antúnez et al., 2009; Aufauvre et al., 2014; Chaimanee et al.,  
67 2012; Dussaubat et al., 2012) and alters pheromone production in worker and queen honey  
68 bees (Alaux et al., 2011; Dussaubat et al., 2010; Holt et al., 2013). Some studies also revealed  
69 that *N. ceranae*-infected honeybees have shorter lifespans than uninfected honeybees  
70 (Alaux et al., 2009; Goblirsch et al., 2013; Higes et al., 2006; Vidau et al., 2011). However, the  
71 presence of *N. ceranae* is not systematically associated with honeybee weakening and

72 mortality (Cox-Foster et al., 2007; Gisder et al., 2010; Invernizzi et al., 2009), suggesting  
73 modulations in the parasite virulence. Possible explanations for this variation include  
74 parasite or host genetics (Chaimanee et al., 2010; Dussaubat et al., 2013; Medici et al., 2012;  
75 Williams et al., 2008), climate (Chen et al., 2012; Gisder et al., 2010), nutrition (Alaux et al.,  
76 2010b; Fleming et al., 2015), or interactions with other stressors such as environmental  
77 contaminants or other parasites. Indeed, some recent studies demonstrated that *N. ceranae*  
78 can sensitize the honeybees to chemical stressors (Alaux et al., 2010a; Aufauvre et al., 2014,  
79 2012; Pettis et al., 2012; Retschnig et al., 2014; Vidau et al., 2011; Wu et al., 2012).

80 In order to explain disorders and detect (early) modifications on bee physiology, we must  
81 acquire molecular tools to screen from genome to metabolome (Lankadurai et al., 2013).  
82 Among these tools, metabolomics is the most informative, looking at the end of the “omic  
83 cascade” for the small metabolites, and strongly linked to the phenotype (Alonso et al.,  
84 2015; Bundy et al., 2008; Fiehn, 2002; Liu and Locasale, 2017). Most of the time, to visualize  
85 a wide range of metabolites, several analytical techniques are required. Mass spectrometry  
86 (MS) is one of the most sensitive and precise technique, depending on mass spectrometer  
87 accuracy, but is limited by chromatographic coupling and in-source ionization. Nuclear  
88 magnetic resonance (NMR) spectroscopy provides the widest coverage of all techniques.  
89 Nevertheless, sensitivity and resolution are regular drawbacks.

90 Untargeted metabolomics has the advantage to highlight both known and unknown  
91 metabolites resulting from phenotypic evolution. Based on statistical filters, all signals from  
92 analytical devices (MS and/or NMR) are examined for possible correlation with the observed  
93 biological effect (Wishart et al., 2008). Those with high correlation will be submitted to  
94 deeper analyses as data/base mining, MS-MS and/or 2-dimensional NMR experiments if  
95 needed, to reveal the identity of the associated biomarker.

96 One of the most established protocols in metabolomics is the metabolic profiling of plasma  
97 (Simón-Manso et al., 2013; Zhao et al., 2010) and urine (Zhang et al., 2012) on “higher  
98 animals”. Biological fluids are easy to collect and store and contain a wide range of  
99 metabolites that can be impacted by many physiological disturbances including medication,  
100 nutrition or disease (Zhang et al., 2020). In this way, researchers aim to find host biomarkers  
101 for early diagnosis of infectious diseases, collect evidence of metabolic disorders along time-  
102 periods or improve nutrition benefits. Hemolymph is the sole biofluid in the insect,  
103 analogous to the blood in invertebrates, and is composed of fluid plasma in which  
104 hemolymph cells (hemocytes) are suspended. It circulates in the interior of the insect body  
105 and remains in direct contact with the animal's tissues. Analyzing this fluid is an opportunity  
106 to access to metabolic pool impacted by stressors (Aliferis et al., 2012; Wang et al., 2019).  
107 Aliferis et al. (2012) previously reported by GC/MS the metabolite profiling of hemolymph in  
108 bees naturally infected by *N. ceranae*. They revealed that a gut parasite can induce a general  
109 disturbance of the honeybee physiology.

110 In our study, we have developed a methodology to perform metabolomics on hemolymph  
111 samples, using combined LC/MS and NMR approaches. The aim was to investigate the  
112 metabolic response of honeybees following experimental infection of emergent bees by *N.*  
113 *ceranae*. Metabolome of the hemolymph was examined in both infected and uninfected  
114 honeybees at two post-infection times.

115

## 116 **2. Materials and methods**

117

### 118 **2.1. Biological experiments**

119

120 **2.1.1. Honeybee artificial rearing**

121 All experiments were performed with a mixture of honeybees taken from three Buckfast  
122 colonies of the same apiary at the Laboratoire Microorganismes : Génome et Environnement  
123 (UMR 6023, Université Clermont Auvergne, France). We confirmed that the three colonies  
124 were free of *Nosema* (sampling of 30 foragers for each colony) by PCR using specific primers  
125 as previously described (Higes et al., 2006). Two frames of sealed brood were placed in an  
126 incubator in the dark at 33°C with 60% relative humidity. Emerging honeybees (100 per  
127 colony) were collected, confined to laboratory Pain-type cages in two groups (infected vs  
128 uninfected, see below for the infection procedure) of 50 individuals, and maintained in the  
129 incubator. During this time, honeybees were fed *ad libitum* with candy (Apifonda®)  
130 supplemented with fresh pollen (Naturapi). In order to mimic the colony environment, a  
131 small piece of wax and a 5-mm piece of Beeboost® (Pherotech, Delta, BC, Canada) releasing  
132 five queen mandibular pheromones, were placed in each cage. Each day, feeders were  
133 replaced; dead bees were counted and removed.

134

135 **2.1.2. Experimental infection with *Nosema ceranae***

136 Spores of *N. ceranae* were obtained from bees experimentally-infected in the laboratory and  
137 the infection process was conducted as previously described (Vidau et al., 2011). Briefly, the  
138 intestinal tract of infected bees was dissected and homogenized in PBS and the resulting  
139 suspension was filtered through Whatman No 1 filter paper, cleaned by centrifugation and  
140 resuspended in PBS. At 5 d post-emergence, caged honeybees were starved for 3 h, CO<sub>2</sub>-  
141 anaesthetized and individually transferred in “infection boxes” consisting of 40 ventilated  
142 compartments (3.5 cm<sup>3</sup>). Each compartment was supplied with a tip containing 125,000  
143 spores of *N. ceranae* diluted in 3 µL of water. “Infection boxes” were placed in the incubator

144 and 1 h later, bees that had consumed the total spore solution were again caged (50 bees per  
145 cage). Uninfected bees were similarly treated without *N. ceranae* spores in the water. At the  
146 end of the experiment, we checked that the control remained uninfected.

147

### 148 **2.1.3. Hemolymph sampling**

149 Hemolymph samples were collected at day 2 (D2) and day 10 (D10) post-inoculation from  
150 both infected and control (uninfected) honeybees using the method described by (Mayack  
151 and Naug, 2010). Bees were first CO<sub>2</sub>-anaesthetized and placed on ice, before antenna  
152 cutting. Immediately, honeybees were placed into PCR tube and centrifuged at 16,000 x *g*  
153 during 30 s. Hemolymph was collected in a new tube and stored at -80°C until analysis.

154

## 155 **2.2. Chemical analyses**

156

### 157 **2.2.1. Chemicals and reagents**

158 Creatinine (Fluka), phenylalanine and tryptophan (Sigma-Aldrich) were used as external  
159 standards for LC/MS quality control. For NMR experiments, Deuterium oxide (D<sub>2</sub>O) was  
160 purchased from Eurisotop and 3-(trimethylsilyl) propionic-2,2,3,3- tetra-d<sub>4</sub> acid sodium salt  
161 (TSP-d<sub>4</sub>) was purchased from Sigma-Aldrich. Acetonitrile (Optima LC-MS), water (Optima LC-  
162 MS) and ammonium acetate (Optima) were purchased from Fisher Scientific for LC/MS  
163 analyses. MS external calibration was performed using lithium hydroxide monohydrate and  
164 formic acid (Fluka).

165

### 166 **2.2.2. Standard solutions and sample preparations for LC/MS and NMR**

167 Stock solutions were prepared for each standard compound (creatinine, phenylalanine and



168 tryptophan) at a concentration of 0.5 mg/ml in water/acetonitrile 1:1 containing 0.1% formic  
169 acid and were stored at -20°C. A mix of all standard solutions was extemporaneously  
170 prepared, for a final concentration of 5 µg/mL. Repeated analyses of the mixed standard  
171 solution ensure system stability before analysis of biological samples. Forty-eight hemolymph  
172 samples (10 µL each, 12 per modality) were diluted in water (LC/MS grade) 1:4 to decrease  
173 viscosity and provide a sufficient volume, considering LC sampling capabilities. Finally, 5 µL  
174 was injected in LC/MS for each analysis. For <sup>1</sup>H-NMR analyses, 51 hemolymph samples (12  
175 bees per modality, but 15 for infected ones at D10) were centrifuged at 14000 x g for 10 min  
176 at 4°C. Three hemolymph samples (from the same experimental condition) were pooled (to  
177 reach the minimum volume required for NMR experiment) and the final volume was  
178 adjusted to 50 µl with D<sub>2</sub>O. The Metabolic Profiler<sup>®</sup> platform robot (Bruker) prepared all  
179 analytical samples by mixing 50 µl of pooled samples with 150 µl of phosphate buffer (1.5 M  
180 phosphate in D<sub>2</sub>O at pH 7.06). D<sub>2</sub>O was used for shimming and locking, whereas TSP-d<sub>4</sub>  
181 constituted a reference for chemical shifts (0 ppm) for NMR. Finally, 180 µl of the solution  
182 was injected, through a capillary, for the online <sup>1</sup>H-NMR profiling. Quality control samples  
183 were also prepared using aliquots from each analytical sample. They ensure system stability  
184 and permit to improve spectra processing.

185

### 186 **2.2.3. Metabolic profiler<sup>®</sup> platform (Bruker Biospin, France)**

187 Ultraperformance liquid chromatography-mass spectrometry (UPLC-MS) used was a  
188 MicroToF system (Bruker) equipped with an electrospray ionization probe (ESI) and a 1200  
189 series chromatographic system (Agilent). Chromatographic separation was performed with a  
190 kinetex HILIC column (100 x 2.1mm, 2.6 µm, Phenomenex) with pre-column. The mobile  
191 phase was composed with acetonitrile (A) and water (B) solvents, both containing 10 mM

192 ammonium acetate. The flow rate was 0.4 mL/min and the gradient elution was carried out  
193 as follows: 0-2 min at 100% A; 2-4 min linear gradient to 80% A; 4-13 min linear gradient to  
194 20% A and back to 100% A into 10 sec (initial conditions); 1 min 50 sec equilibration wash  
195 with 100% A, for a total run of 15 min. The injection volumes for both samples and standards  
196 were 5  $\mu$ L and the column temperature was set at 25°C. Blanks of pure water and pure  
197 acetonitrile were injected after every 10 hemolymph samples, for cleaning the  
198 chromatographic system. The mass spectrometer was calibrated with lithium formate  
199 clusters (5 mM into water) and operated in positive ion mode for full scan (50-1000 m/z)  
200 detection. Nitrogen was used as the nebulizer and the drying gas. The nebulizer pressure was  
201 2 bars, the desolvation gas flow rate was 8 L/min and desolvation temperature was  
202 maintained at 200°C. Capillary tension was 4000 V.

203 On flow 1-dimensional  $^1\text{H}$ -NMR experiments were done on an Avance III 500 MHz NMR  
204 spectrometer, using an inflow 3-mm FISEI z-gradient ( $^1\text{H}$ - $^{13}\text{C}$ ) probe with a 60- $\mu$ l cell.  
205 A standard one dimensional noe spectroscopy sequence (noesygppr1d with water  
206 presaturation and gradients) was used with low power irradiation of the water resonance  
207 during the recycle delay of 4 s and the mixing time of 10 ms. 256 scans were collected with  
208 an 90° impulsion time of 9.29  $\mu$ s, an acquisition time of 3.28 s, a spectral window of 10000  
209 Hz and 64K data points zero-filled to 128K before Fourier transformation with 0.3 Hz line  
210 broadening. All NMR spectra were recorded at 300K and processed with Topspin version 2.1.

211

#### 212 ***2.2.4. Ultraperformance liquid chromatography-tandem mass spectrometry (UPLC-MS-MS)***

213 For identification purposes, a few samples from each condition, and that were representative  
214 for the features in the model, were analysed in full scan (80-1000 m/z) for positive ion mode  
215 on an LTQ Orbitrap Velos MS with same chromatographic conditions (gradient, column) as for

216 UPLC-MS profiling. The m/z of each feature was searched in the resulting chromatograms to  
217 obtain a better mass accuracy of the features, which was used to determine the most  
218 probable molecular formulae. The parent ion was identified from in-source fragments and  
219 adducts, and additional structural information on the features was obtained by performing  
220 MS/MS fragmentation on relevant ions using MS-MS in product ion scan mode with collision  
221 energies of 10, 20, and 30 eV. All information on the features was used to search into  
222 chemicals and metabolites databases (cf. § 2.5.3).

223

#### 224 **2.2.5. 1D and 2D NMR experiments for metabolite identification**

225 For the metabolite identification step, the sample corresponded to a pool of 25 hemolymphs  
226 (mix of both infected and uninfected bees). The total volume of hemolymph (300 µl) was  
227 mixed with 300 µl of phosphate buffer in D<sub>2</sub>O. The NMR spectrometer used (TGIR - CNRS de  
228 Gif/Yvette) was a Bruker Avance III 950 MHz equipped with a cryoprobe (1.7, 3 and 5 mm  
229 tube) TCI (<sup>1</sup>H/<sup>13</sup>C/<sup>15</sup>N/<sup>2</sup>H) with z-gradient coil probe (Bruker Biospin Wissenbourg, France).

230 For 1D <sup>1</sup>H-Spectra, a standard one dimensional noe spectroscopy sequence (noesygppr1d  
231 with water presaturation and gradients) was used with low power irradiation (31 µW) of the  
232 water resonance during the recycle delay of 10 s and the mixing time of 10 ms. 128 scans  
233 were collected with a 90° impulsion time of 8.1 µs, an acquisition time of 3.3 s, a spectral  
234 window of 10000 Hz and 64K data points zero-filled to 128K before Fourier transformation  
235 with 0.3 Hz line broadening. For 2D homonuclear (COSY TOCSY, JRES) and heteronuclear  
236 (<sup>1</sup>H/<sup>13</sup>C HSQC and HMBC) experiments were performed with quadrature phase detection in  
237 dimensions, using state-TPPI or QF detection mode in the indirect one. For each 512 (80 for  
238 JRES) increments in the indirect dimension, 2K data points (8K for JRES) were collected and  
239 16 transients were accumulated in the direct dimension. <sup>13</sup>C decoupling (GARP) was

240 performed during acquisition time for heteronuclear experiments. A  $\pi/2$  shifted square sine-  
241 bell function was applied in the two dimensions before Fourier transformation. Spectra were  
242 treated with Topspin version 3.1. All NMR spectra were recorded at 300K.

243

### 244 **2.3. Data management**

245

#### 246 **2.3.1. Data extraction**

247 MS data were converted into NetCDF format and extracted to data matrix using XCMS  
248 package under R environment (v. 2.15.3). Briefly, after ion extraction (m/z), a retention time  
249 (RT) correction was performed before production of the matrix including for each ion  
250 (m/z@RT) the relative intensity (area) detected into each analytical sample. Finally, CAMERA  
251 package (Kuhl et al., 2012) proposed a first annotation according to common adducts and  
252 natural isotopes. NMR data were binned using AMIX software (v. 3.9.10, Bruker) after  
253 alignment and baseline correction. Extraction process was chosen as follows: fixed bucketing  
254 of 0.01 ppm, from 0.13 to 10 ppm; solvent signal exclusion between 4.7 and 4.9 ppm; signals  
255 integration on the sum of intensities; normalization on total intensity. The resulting matrix  
256 was used for statistics.

257

#### 258 **2.3.2. Statistical analyses**

259 Multivariate analyses were performed using SIMCA-P+ (v. 12.0.1.0, Umetrics) for non-  
260 supervised (PCA) and supervised ((O)PLS-DA) methods. Two normalization methods were  
261 tested, univariate (UV) and pareto (PAR), in order to obtain the most robust statistical  
262 models. All statistical models were validated according to explanatory ( $R^2$ ) and predictive  
263 ( $Q^2$ ) values as well as with random permutations. Lists of signals (ions or buckets) were

264 selected for each model according to VIP (variable importance in projection) scores (>1). For  
265 all valid models, a list of ions considered to be the most implicated was selected, according  
266 to VIP score. Univariate analyses were performed on Excel software (Windows) for ANOVA  
267 filtering on MS data. ANOVA multiway, with interaction, was performed in order to separate  
268 analytical effects from biological ones and to distinguish, when possible, age and infection  
269 metabolic effects.

270

### 271 **2.3.3. Metabolite identification**

272 Identification of VIP ions was performed manually or using R script for data mining on  
273 several public metabolic databases (KEGG, MetaCyc, HMDB). MS-MS fragmentation features  
274 were compared to MassFrontier (v. 7; ThermoScientific) theoretical schemes and databases  
275 (MassBank, METLIN, HMDB, PRIME). NMR VIP signals (buckets) were attributed manually  
276 using previously published data (Fan, 1996; Nicholson et al., 1995; Willker et al., 1996) and  
277 the human metabolome public database (HMDB).

278

## 279 **3. Results**

280 For metabolic profiling, hemolymph samples from both uninfected (UI) and *N. ceranae*-  
281 infected (I) bees were collected at two time points considered as early (D2) and late (D10)  
282 times of infection, respectively. Forty eight samples (12 for each modality) were individually  
283 analyzed by LC-MS in two batches (23 samples for batch 1 and 25 samples for batch 2). For  
284 <sup>1</sup>H-NMR experiments, hemolymph from 51 bees were pooled in 17 groups of three.

285

### 286 **3.1. LC-MS profiles and metabolite identification**

287 All hemolymph samples analyzed by LC-MS showed similar “total ion chromatogram”  
288 profiles (**Suppl. Fig. 1**). Multivariate models were then applied to measure age (D2 vs D10)  
289 and treatment (I vs UI) effects from a data matrix of 1294 ions. Among each analytical batch,  
290 PLS-DA models clearly showed that the age of bees remained the parameter with the  
291 strongest effect (**Figure 1**) and no statistical model was valid considering the infection effect  
292 only. ANOVA filtering permitted discrimination between batch effect and combined effect of  
293 age and infection, and all ions with a p-value above 0.05 were eliminated. A final list of 15  
294 ions according to VIP scores, with levels significantly up- or down-regulated (at D2 and/or  
295 D10), was then used for metabolite identification. Eight metabolites, corresponding to  
296 potential biomarkers representative of infection alone or combined effect of age and  
297 infection, were accurately identified according to spectral data and/or standard comparisons  
298 (**Table 1**). These biomarkers included 3 dipeptides (Glu-Thr, Cys-Cys and  $\gamma$ -Glu-Leu/Ile), one  
299 amino acid (histidine), one amino sugar (hexosamine), two metabolites involved in lipid  
300 metabolism (glycerophosphocholine and O-Phosphorylethanolamine) and ethyl aconitate, a  
301 tricarboxylic acid derivative, listed as flavoring agent. For each selected marker,  
302 infected/uninfected (I/UI) ratios were mentioned at both D2 and D10 post-infection times.  
303 The most interesting metabolite was hexosamine. In hemolymph of infected bees, the  
304 circulating amount of hexosamine was 3x lower at D2 and 7-8x higher at D10 compared to  
305 the control (**Table 1**). Similarly, in infected bees compared to control, levels of circulating  
306 histidine and another “amino acid-like” putative compound were lower at D2 and higher at  
307 D10. Three other metabolites (glycerophosphocholine and two dipeptides, Cys-Cys and Glu-  
308 Thr) exhibited an opposite pattern. These circulating metabolites were more abundant at D2  
309 and lower at D10. O-phosphorylethanolamine, a “sulfur-containing” putative metabolite and  
310 peptides ( $\gamma$ -Glu-Leu/Ile and another putative “short peptide”) were detected at higher levels

311 in the hemolymph of infected bees at D2 and D10. Finally, ethyl aconitate, levels of  
312 circulating “carbohydrate-like” and “amine-like” putative compounds were lower in infected  
313 bees than in control bees, at the two time points post-infection.

314

### 315 **3.2. NMR profiles and metabolite identification**

316 Each NMR spectrum was obtained from a pool of hemolymphs from three honeybees.  
317 Spectra analysis showed signal richness of both aliphatic and sugar zones, below 5 ppm  
318 (**Suppl. Fig. 2**). Using multivariate statistical analysis tools, we observed a strong effect of  
319 ageing with PCA and PLS-DA models (**Figure 2**). Similar to MS results, age had the strongest  
320 effect and no valid model was obtained when considering the infection parameter alone.  
321 Buckets were selected according to VIP score (above 0.99). Eight biomarkers were clearly  
322 identified, according to spectral data and databases comparisons, and I/NI ratios were  
323 calculated at both D2 and D10 (**Table 2**). These biomarkers included four carbohydrates  
324 (fructose and glucose, both  $\alpha$  and  $\beta$  forms), one amino acid (proline), a polyamine compound  
325 (spermidine) and two metabolites involved in lipid metabolism (choline and  
326 glycerophosphocholine). Signals for carbohydrates (fructose and glucose) shared similar  
327 behaviors. These compounds were more abundant in the hemolymph of infected bees  
328 particularly at the early infection time (D2). In contrast, proline was always less abundant in  
329 infected hemolymph. As for the MS data, levels of circulating glycerophosphocholine were  
330 higher in the hemolymph of infected bees at D2, then decreased at D10. Choline showed a  
331 completely opposite pattern. Although the amount of spermidine decreased at D2 for  
332 infected bees, no significant difference was observed at D10 between I and UI samples.

333

### 334 **4. Discussion**

335

336 **4.1. Biological sampling**

337 This proof of concept study was performed to develop transposable methodologies for  
338 metabolic profiling on honeybee hemolymph from bees in hives and was linked to a study of  
339 experimental infection of caged honeybees by the gut parasite *N. ceranae* conducted to  
340 reveal metabolic shifts during the infectious process. We also raised several questions about  
341 the quality and variability of biological samples.

342 Experimental results have suggested difficulties in assessing the health status of honeybees  
343 from hives in field conditions. Both biotic and abiotic stressors may produce effects on the  
344 physiology of the bees and modify the metabolic pool. Even using molecular biology (RNA  
345 seq and/or qPCR) and analytical (multiresidue detection) tools, it is too time consuming and  
346 costly to evaluate unstressed bees (*i.e.* healthy bees). Only visual symptoms and mortality  
347 were evaluated during the experiment. In our opinion, difficulty in obtaining clear signatures  
348 of *Nosema* infection in natural populations are partly due to honeybee genetic variability.  
349 For example, Kurze et al. (2015) demonstrated that *Nosema*-tolerant honeybees were able  
350 to escape the manipulation of apoptosis by the parasite. In addition, when a study follows  
351 mortality across time, the major risk in sampling surviving bees is to artificially select  
352 resistant insects with low-level infections or those less sensitive to infection (*e.g.* genetic  
353 tendencies). However, even if honeybees are generally stressed by various factors, our study  
354 should reveal the metabolic impact of the infection.

355 Finally, other limitations for biological sampling could be the drastic treatments for bee  
356 infection, CO<sub>2</sub> anesthesia and hemolymph harvesting. In order to prevent any  
357 artificial/technical disruptions, following a rigorous protocol is mandatory (“The



358 Metabolomics Standards Initiative (MSI) and Core Information for Metabolomics Reporting  
359 (CIMR),” n.d.).

360

#### 361 **4.2. Analytical experiments**

362 Discriminating metabolic disturbances is an important issue in metabolomics. Firstly,  
363 metabolic coverage, in term of quality and quantity, is strongly linked to analytical tools.  
364 Mass spectrometry did not permit easy distinction of isobaric metabolites with similar  
365 fragmentation schemes. For this reason, based on our data, it was not possible to distinguish  
366 Ile/Leu containing compounds or reveal which hexosamine(s) is (are) impacted. Some NMR  
367 signals for ratio calculation were mixed in the same bucket and, thus, polluted. For that  
368 reason, they were discarded from our list (e.g. other fructose signals; data not shown). For  
369 these reasons, hyphenation using LC-MS, GC-MS and/or NMR is one of the best ways to  
370 harvest information, as precisely as possible (Wishart et al., 2008).

371 Secondly, with a very large amount of metabolic signals, data treatments and statistics are  
372 required to filter and reveal significant elements before any identification efforts (Monnerie  
373 et al., 2019). In our study, combining LC-MS and NMR metabolomics datasets improved  
374 coverage of the metabolome. Processing workflows (R packages; (Giacomoni et al., 2015)  
375 are time consuming but ensure data reproducibility and comparability. The differences in the  
376 metabolome profiles were deciphered using multivariate statistics (PLS-DA). Many statistical  
377 tools are able to manage such datasets, but multidimensional representations permit  
378 maintenance of data integrity and complexity. Such approach reveals, at the same time, the  
379 variability of the complete dataset and the group of signals that are most relevant  
380 considering the scientific hypothesis (Boccard and Rudaz, 2014). Analytical redundancy (e.g.

381 hexosamine in MS; Choline and spermidine in NMR) and metabolic interaction are keys for  
382 the explanation of such statistical effects and reinforce the identification of biomarkers.  
383 Finally, LC-MS-MS as well as 2D-NMR enhanced the identification of biomarkers. They are  
384 low throughput experiments, mostly targeted on the few signals of interest, but increase the  
385 quality of the identification. Data mining should be time consuming depending on what kind  
386 of metabolite is highlighted. The well-known primary metabolite is quickly identified; those  
387 less documented will take time to be identified with certainty. But guessing for “*de novo*”  
388 identification (no information in databases) requires high resolution analytical experiments  
389 to succeed.

390

#### 391 ***4.3. Biomarkers of the infection and impacts on honeybee metabolism***

392 Because hemolymph is the sole biofluid which circulates in the interior of arthropod body,  
393 we can infer that the metabolome of a hemolymph sample reflects the exchanges occurring  
394 between organs (digestive, neural, reproductive, etc.) during the infectious process. As  
395 expected, the age of bees was the parameter with the strongest effect on the hemolymph  
396 metabolome. However, we succeeded in identifying 15 metabolites that were assigned as  
397 candidate biomarkers representative of infection alone or the combined effect of age and  
398 infection. The levels of these metabolites could be interpreted as either a deleterious impact  
399 of infectious process or a defensive response against the pathogen.

400 The same pattern was observed for O-phosphorylethanolamine (PE), the dipeptide Glu-  
401 Leu/Ile, glucose and fructose ( $\alpha$  and  $\beta$  forms). These metabolites were more abundant in the  
402 hemolymph of infected bees, particularly at D2 post-infection. Glycerophosphocholine (GPC;  
403 one major form of choline storage) identified by both LC-MS and NMR, as well as two other  
404 dipeptides (Cys-Cys and Glu-Thr), were also increased in infected samples but only at early

405 time of infection (D2). These observations could be related to impacts on proteins as  
406 building blocks and glycerophospholipid used in nervous and parasympathic systems.  
407 Infection is known to increase energetic demand and modify behavior in *N. ceranae*-infected  
408 bees (Alaux et al., 2010a; Martín-Hernández et al., 2011; Mayack and Naug, 2009; Naug and  
409 Gibbs, 2009). Some dipeptides also are known to have physiological or cell-signaling effects,  
410 although most are simply short-lived intermediates on their way to specific amino acid  
411 degradation pathways following further proteolysis. Some recent studies showed that lipid  
412 depletion is a phenomenon strongly linked to pathogen development (Franchet et al., 2019;  
413 Li et al., 2018). The level of amino acids and spermidine was lower in *Nosema*-exposed  
414 samples at D2 post-infection, whereas an antagonistic pattern occurred at D10 between  
415 proline and histidine. Decreased levels of amino acids, including proline, were also observed  
416 by (Aliferis et al., 2012) in the hemolymph of bees naturally infected by *N. ceranae*.  
417 Spermidine seems to be unmodified at D10. Proline and spermidine are involved in a key  
418 pathway, the arginine and proline pathway, at the boundary of important metabolisms  
419 (amino acids, glutathione, polyamine, etc.). Proline, the dipeptide Glu-Thr and GPC  
420 decreased at D10. The level of proline decreased as well in infected bees at D2 while the  
421 others increased. Hexosamine, the amino acid histidine and the amino alcohol choline  
422 showed a different pattern. The levels of these three metabolites were lower in infected  
423 bees at D2 and higher at D10 when compared to uninfected bees. Hexosamine may lead to  
424 the biosynthesis of chitin, one of the essential components of insect cuticle and peritrophic  
425 matrix in the gut. The peritrophic matrix lines the midgut of most insects and is a protective  
426 barrier against microbial infections (Kelkenberg et al., 2015). Chitin is also a major  
427 component of the cell wall of microsporidian spores (Bigliardi et al., 1996). Some studies  
428 revealed a degeneration of the peritrophic membrane in bees infected by *N. ceranae*

429 (Dussaubat et al., 2012). Thus, the higher level of hexosamine detected in the hemolymph of  
430 infected bees at D10 could be the result of degradation of the peritrophic matrix during the  
431 infectious process.

432

### 433 **CONCLUSION**

434 This study is the first presenting a complete methodology to analyze bee hemolymph using  
435 the up-to-date technologies for metabolomics, MS and NMR. The aim of our study was to  
436 detect signatures of the pathological processes during the infection of bees by the gut  
437 parasite *N. ceranae*. As a proof of concept, we identified biomarkers that could be useful for  
438 a better understanding of pathophysiological mechanisms of the honeybee infection by *N.*  
439 *ceranae*.

440 For further experiments, we recommend evaluation of the identified biomarkers, through  
441 precise quantification, on workers from hives under different field conditions. This  
442 untargeted metabolomic approach could also be used to identify biomarkers in the gut  
443 during the progression of the infection. In order to reduce disturbances related to other  
444 biotic or abiotic factors, we propose to use hives under insect mesh tunnels and follow  
445 health status of colonies through random testing.

446

### 447 **Acknowledgement:**

448 This work was funded by grants from the French National Research Agency (ANR, grant  
449 number ANR-12-BSV3-0020) and received support from PIA METABOHUB (ANR-AA-INSB-  
450 0010) and TGIR-RMN (IR-RMN-THC Fr3050 CNRS).

451

### 452 **Figure captions**

453

454 **Figure 1. PLS-DA on LC/MS profiles.** Batch 1 with 23 analyses (1), Batch 2 with 25 analyses  
455 (2). Box for Day 2, dot for Day 10, blue figure for uninfected samples and red for infected  
456 ones. A strong age effect is shown on the two batches (dashed black line). (1) PC1 (25,7%)  
457 and PC2 (18,3%), (2) PC1 (20,9%) and PC2 (12,4%); Hotelling T2 (ellipse) = 95%.

458

459 **Figure 2. PLS-DA on NMR data.** Box for Day 2, dot for Day 10, blue figure for uninfected  
460 samples and red for infected ones. An age effect is shown on the model (dashed black line).  
461 PC1 (44,8%) and PC2 (14,1%); Hotelling T2 (ellipse) = 95%.

462

463 **Table 1: Putative biomarkers identified from LC-MS and MS-MS experiments;** ID was  
 464 obtained from XCMS package (p for positive ionization; first number as mass on charge  
 465 measurement; T for retention time; second number as the retention time of the ion in  
 466 minutes). Infected/Uninfected (I/UI) ratios, at two time points (Day 2 and Day 10), were  
 467 calculated on data matrix (relative intensities). Candidate names were proposed according  
 468 to data obtained by LC-MS and MS-MS analyses and compared with databases and/or  
 469 standards. ANOVA filtering distinguished between biomarkers linked to infection only (I) or  
 470 to both infection and age (II). Signals were identified according to a mass precision less than  
 471 1 ppm, except for \* 5 ppm far and \*\* 20 ppm far.

ID	I/UI @ D2	I/UI @ D10	Putative name	ANOVA
p133,058T6,3	0,14	1,55	Aminoacid like	I
p142,03T8,2	1,81	1,40	O-Phosphorylethanolamine	I
p179,054T6,4	0,45	0,63	Carbohydrate like	I
p203,059T5,7	0,42	0,86	Ethyl aconitate **	I
p246,249T5,8	0,84	0,36	Amine like	I
p251.044T6.3	1,17	3,40	Sulfur containing	I
p261,045T7,1	4,75	3,09	$\gamma$ -Glu-Leu, $\gamma$ -Glu-Ile	I
p399,134T8,2	2,84	1,67	Short (tri or tetra-) peptide	I
p145,052T5,6	0,36	8,57	Fragment of hexosamine	II
p156,078T8,7	0,52	1,18	Histidine	II
p180,093T5,6	0,38	6,64	Hexosamine	II
p181,092T5,6	0,34	7,26	13C of hexosamine	II
p225,035T6,3	2,38	0,41	Cys-Cys *	II
p249,113T6,9	1,47	0,36	Glu-Thr	II
p280,102T8,3	1,21	0,45	Glycerophosphocholine	II

472  
 473

474

475 **Table 2: Putative metabolite biomarkers identified from NMR experiments;** ID was  
476 obtained with AMIX software (the center of each bucket), and Infected/Uninfected (I/UI)  
477 ratios, at the two time points (Day 2 and Day 10), were calculated on extracted matrix  
478 (relative intensities). Candidate names were proposed according to Identification realized  
479 using previously published data and web databases.

ID	I/UI @ D2	I/UI @ D10	Putative name
3.205	0,60	1,16	Choline
3.225	2,04	0,74	GPC
4.005	1,68	1,19	$\alpha$ -Fructose
4.015	1,75	1,17	$\beta$ -Fructose
4.135	0,81	0,67	Proline
4.115	1,63	1,12	$\alpha$ -Fructose
3.215	1,81	0,82	GPC
3.055	0,84	1,00	Spermidine
1.775	0,85	0,98	Spermidine
1.765	0,87	1,02	Spermidine
3.045	0,84	0,99	Spermidine
5.235	1,15	1,05	$\alpha$ -Glucose
3.195	0,59	1,19	Choline
1.785	0,79	0,95	Spermidine
3.515	0,78	1,10	Choline
3.065	0,85	0,99	Spermidine
4.645	1,12	1,04	$\beta$ -Glucose

480

481

482

- 484  
485  
486 Alaux, C., Brunet, J.-L., Dussaubat, C., Mondet, F., Tchamitchan, S., Cousin, M., Brillard, J., Baldy, A.,  
487 Belzunces, L.P., Conte, Y.L., 2010a. Interactions between *Nosema* microspores and a  
488 neonicotinoid weaken honeybees (*Apis mellifera*). *Environ. Microbiol.* 12, 774–782.  
489 <https://doi.org/10.1111/j.1462-2920.2009.02123.x>
- 490 Alaux, C., Ducloz, F., Crauser, D., Le Conte, Y., 2010b. Diet effects on honeybee immunocompetence.  
491 *Biol. Lett.* 6, 562–565. <https://doi.org/10.1098/rsbl.2009.0986>
- 492 Alaux, C., Folschweiller, M., McDonnell, C., Beslay, D., Cousin, M., Dussaubat, C., Brunet, J.-L., Conte,  
493 Y.L., 2011. Pathological effects of the microsporidium *Nosema ceranae* on honey bee queen  
494 physiology (*Apis mellifera*). *J. Invertebr. Pathol.* 106, 380–385.  
495 <https://doi.org/10.1016/j.jip.2010.12.005>
- 496 Alaux, C., Sinha, S., Hasadsri, L., Hunt, G.J., Guzmán-Novoa, E., DeGrandi-Hoffman, G., Uribe-Rubio,  
497 J.L., Southey, B.R., Rodriguez-Zas, S., Robinson, G.E., 2009. Honey bee aggression supports a  
498 link between gene regulation and behavioral evolution. *Proc. Natl. Acad. Sci.* 106, 15400–  
499 15405. <https://doi.org/10.1073/pnas.0907043106>
- 500 Aliferis, K.A., Copley, T., Jabaji, S., 2012. Gas chromatography–mass spectrometry metabolite  
501 profiling of worker honey bee (*Apis mellifera* L.) hemolymph for the study of *Nosema*  
502 *ceranae* infection. *J. Insect Physiol.* 58, 1349–1359.  
503 <https://doi.org/10.1016/j.jinsphys.2012.07.010>
- 504 Alonso, A., Marsal, S., Julià, A., 2015. Analytical Methods in Untargeted Metabolomics: State of the  
505 Art in 2015. *Front. Bioeng. Biotechnol.* 3. <https://doi.org/10.3389/fbioe.2015.00023>
- 506 Antúnez, K., Martín-Hernández, R., Prieto, L., Meana, A., Zunino, P., Higes, M., 2009. Immune  
507 suppression in the honey bee (*Apis mellifera*) following infection by *Nosema ceranae*  
508 (*Microsporidia*). *Environ. Microbiol.* 11, 2284–2290. <https://doi.org/10.1111/j.1462-2920.2009.01953.x>
- 510 Aufauvre, J., Biron, D.G., Vidau, C., Fontbonne, R., Roudel, M., Diogon, M., Viguès, B., Belzunces, L.P.,  
511 Delbac, F., Blot, N., 2012. Parasite-insecticide interactions: a case study of *Nosema ceranae*  
512 and fipronil synergy on honeybee. *Sci. Rep.* 2, 1–7. <https://doi.org/10.1038/srep00326>
- 513 Aufauvre, J., Misme-Aucouturier, B., Viguès, B., Texier, C., Delbac, F., Blot, N., 2014. Transcriptome  
514 Analyses of the Honeybee Response to *Nosema ceranae* and Insecticides. *PLoS ONE* 9.  
515 <https://doi.org/10.1371/journal.pone.0091686>
- 516 Bigliardi, E., Selmi, M.G., Lupetti, P., Corona, S., Gatti, S., Scaglia, M., Sacchi, L., 1996. Microsporidian  
517 Spore Wall: Ultrastructural Findings on *Encephalitozoon hellem* Exospore. *J. Eukaryot.*  
518 *Microbiol.* 43, 181–186. <https://doi.org/10.1111/j.1550-7408.1996.tb01388.x>
- 519 Boccard, J., Rudaz, S., 2014. Harnessing the complexity of metabolomic data with chemometrics. *J.*  
520 *Chemom.* 28, 1–9. <https://doi.org/10.1002/cem.2567>
- 521 Bundy, J.G., Davey, M.P., Viant, M.R., 2008. Environmental metabolomics: a critical review and future  
522 perspectives. *Metabolomics* 5, 3. <https://doi.org/10.1007/s11306-008-0152-0>
- 523 Chaimanee, V., Chantawannakul, P., Chen, Y., Evans, J.D., Pettis, J.S., 2012. Differential expression of  
524 immune genes of adult honey bee (*Apis mellifera*) after inoculated by *Nosema ceranae*. *J.*  
525 *Insect Physiol.* 58, 1090–1095. <https://doi.org/10.1016/j.jinsphys.2012.04.016>
- 526 Chaimanee, V., Warrit, N., Chantawannakul, P., 2010. Infections of *Nosema ceranae* in four different  
527 honeybee species. *J. Invertebr. Pathol.* 105, 207–210.  
528 <https://doi.org/10.1016/j.jip.2010.06.005>
- 529 Chen, Y.-W., Chung, W.-P., Wang, C.-H., Solter, L.F., Huang, W.-F., 2012. *Nosema ceranae* infection  
530 intensity highly correlates with temperature. *J. Invertebr. Pathol.* 111, 264–267.  
531 <https://doi.org/10.1016/j.jip.2012.08.014>



532 Cox-Foster, D.L., Conlan, S., Holmes, E.C., Palacios, G., Evans, J.D., Moran, N.A., Quan, P.-L., Briese, T.,  
533 Hornig, M., Geiser, D.M., Martinson, V., vanEngelsdorp, D., Kalkstein, A.L., Drysdale, A., Hui,  
534 J., Zhai, J., Cui, L., Hutchison, S.K., Simons, J.F., Egholm, M., Pettis, J.S., Lipkin, W.I., 2007. A  
535 Metagenomic Survey of Microbes in Honey Bee Colony Collapse Disorder. *Science* 318, 283–  
536 287. <https://doi.org/10.1126/science.1146498>

537 Dussaubat, C., Brunet, J.-L., Higes, M., Colbourne, J.K., Lopez, J., Choi, J.-H., Martín-Hernández, R.,  
538 Botías, C., Cousin, M., McDonnell, C., Bonnet, M., Belzunces, L.P., Moritz, R.F.A., Le Conte, Y.,  
539 Alaux, C., 2012. Gut Pathology and Responses to the Microsporidium *Nosema ceranae* in the  
540 Honey Bee *Apis mellifera*. *PLoS ONE* 7. <https://doi.org/10.1371/journal.pone.0037017>

541 Dussaubat, C., Maisonnasse, A., Alaux, C., Tchamitchan, S., Brunet, J.-L., Plettner, E., Belzunces, L.P.,  
542 Le Conte, Y., 2010. *Nosema* spp. Infection Alters Pheromone Production in Honey Bees (*Apis*  
543 *mellifera*). *J. Chem. Ecol.* 36, 522–525. <https://doi.org/10.1007/s10886-010-9786-2>

544 Dussaubat, C., Sagastume, S., Gómez-Moracho, T., Botías, C., García-Palencia, P., Martín-Hernández,  
545 R., Le Conte, Y., Higes, M., 2013. Comparative study of *Nosema ceranae* (Microsporidia)  
546 isolates from two different geographic origins. *Vet. Microbiol.* 162, 670–678.  
547 <https://doi.org/10.1016/j.vetmic.2012.09.012>

548 Fan, T.W.-M., 1996. Metabolite profiling by one- and two-dimensional NMR analysis of complex  
549 mixtures. *Prog. Nucl. Magn. Reson. Spectrosc.* 28, 161–219. [https://doi.org/10.1016/0079-](https://doi.org/10.1016/0079-6565(95)01017-3)  
550 [6565\(95\)01017-3](https://doi.org/10.1016/0079-6565(95)01017-3)

551 Fiehn, O., 2002. Metabolomics--the link between genotypes and phenotypes. *Plant Mol. Biol.* 48,  
552 155–171.

553 Fleming, J.C., Schmehl, D.R., Ellis, J.D., 2015. Characterizing the Impact of Commercial Pollen  
554 Substitute Diets on the Level of *Nosema* spp. in Honey Bees (*Apis mellifera* L.). *PLOS ONE* 10,  
555 e0132014. <https://doi.org/10.1371/journal.pone.0132014>

556 Franchet, A., Niehus, S., Caravello, G., Ferrandon, D., 2019. Phosphatidic acid as a limiting host  
557 metabolite for the proliferation of the microsporidium *Tubulosema ratisbonensis* in  
558 *Drosophila* flies. *Nat. Microbiol.* 4, 645–655. <https://doi.org/10.1038/s41564-018-0344-y>

559 Fries, I., 2010. *Nosema ceranae* in European honey bees (*Apis mellifera*). *J. Invertebr. Pathol.* 103,  
560 S73–S79. <https://doi.org/10.1016/j.jip.2009.06.017>

561 Giacomoni, F., Le Corguillé, G., Monsoor, M., Landi, M., Pericard, P., Pétéra, M., Duperier, C.,  
562 Tremblay-Franco, M., Martin, J.-F., Jacob, D., Goulitquer, S., Thévenot, E.A., Caron, C., 2015.  
563 Workflow4Metabolomics: a collaborative research infrastructure for computational  
564 metabolomics. *Bioinformatics* 31, 1493–1495.  
565 <https://doi.org/10.1093/bioinformatics/btu813>

566 Gisder, S., Hedtke, K., Möckel, N., Frielitz, M.-C., Linde, A., Genersch, E., 2010. Five-Year Cohort Study  
567 of *Nosema* spp. in Germany: Does Climate Shape Virulence and Assertiveness of *Nosema*  
568 *ceranae*? *Appl. Environ. Microbiol.* 76, 3032–3038. <https://doi.org/10.1128/AEM.03097-09>

569 Goblirsch, M., Huang, Z.Y., Spivak, M., 2013. Physiological and Behavioral Changes in Honey Bees  
570 (*Apis mellifera*) Induced by *Nosema ceranae* Infection. *PLOS ONE* 8, e58165.  
571 <https://doi.org/10.1371/journal.pone.0058165>

572 Goulson, D., Nicholls, E., Botías, C., Rotheray, E.L., 2015. Bee declines driven by combined stress from  
573 parasites, pesticides, and lack of flowers. *Science* 347.  
574 <https://doi.org/10.1126/science.1255957>

575 Higes, M., Martín, R., Meana, A., 2006. *Nosema ceranae*, a new microsporidian parasite in honeybees  
576 in Europe. *J. Invertebr. Pathol.* 92, 93–95. <https://doi.org/10.1016/j.jip.2006.02.005>

577 Higes, M., Meana, A., Bartolomé, C., Botías, C., Martín-Hernández, R., 2013. *Nosema ceranae*  
578 (Microsporidia), a controversial 21st century honey bee pathogen. *Environ. Microbiol. Rep.* 5,  
579 17–29. <https://doi.org/10.1111/1758-2229.12024>

580 Holt, H.L., Aronstein, K.A., Grozinger, C.M., 2013. Chronic parasitization by *Nosema* microsporidia  
581 causes global expression changes in core nutritional, metabolic and behavioral pathways in  
582 honey bee workers (*Apis mellifera*). *BMC Genomics* 14, 799. [https://doi.org/10.1186/1471-](https://doi.org/10.1186/1471-2164-14-799)  
583 [2164-14-799](https://doi.org/10.1186/1471-2164-14-799)

584 Invernizzi, C., Abud, C., Tomasco, I.H., Harriet, J., Ramallo, G., Campá, J., Katz, H., Gardiol, G.,  
585 Mendoza, Y., 2009. Presence of *Nosema ceranae* in honeybees (*Apis mellifera*) in Uruguay. *J.*  
586 *Invertebr. Pathol.* 101, 150–153. <https://doi.org/10.1016/j.jip.2009.03.006>  
587 Kelkenberg, M., Odman-Naresh, J., Muthukrishnan, S., Merzendorfer, H., 2015. Chitin is a necessary  
588 component to maintain the barrier function of the peritrophic matrix in the insect midgut.  
589 *Insect Biochem. Mol. Biol.* 56, 21–28. <https://doi.org/10.1016/j.ibmb.2014.11.005>  
590 Kuhl, C., Tautenhahn, R., Böttcher, C., Larson, T.R., Neumann, S., 2012. CAMERA: An integrated  
591 strategy for compound spectra extraction and annotation of LC/MS data sets. *Anal. Chem.*  
592 84, 283. <https://doi.org/10.1021/ac202450g>  
593 Kurze, C., Conte, Y.L., Dussaubat, C., Erler, S., Kryger, P., Lewkowski, O., Müller, T., Widder, M.,  
594 Moritz, R.F.A., 2015. *Nosema* Tolerant Honeybees (*Apis mellifera*) Escape Parasitic  
595 Manipulation of Apoptosis. *PLOS ONE* 10, e0140174.  
596 <https://doi.org/10.1371/journal.pone.0140174>  
597 Lankadurai, B.P., Nagato, E.G., Simpson, M.J., 2013. Environmental metabolomics: an emerging  
598 approach to study organism responses to environmental stressors. *Environ. Rev.* 21, 180–  
599 205. <https://doi.org/10.1139/er-2013-0011>  
600 Li, W., Chen, Y., Cook, S.C., 2018. Chronic *Nosema ceranae* infection inflicts comprehensive and  
601 persistent immunosuppression and accelerated lipid loss in host *Apis mellifera* honey bees.  
602 *Int. J. Parasitol.* 48, 433–444. <https://doi.org/10.1016/j.ijpara.2017.11.004>  
603 Liu, X., Locasale, J.W., 2017. Metabolomics: A Primer. *Trends Biochem. Sci.* 42, 274–284.  
604 <https://doi.org/10.1016/j.tibs.2017.01.004>  
605 Martín-Hernández, R., Botías, C., Barrios, L., Martínez-Salvador, A., Meana, A., Mayack, C., Higes, M.,  
606 2011. Comparison of the energetic stress associated with experimental *Nosema ceranae* and  
607 *Nosema apis* infection of honeybees (*Apis mellifera*). *Parasitol. Res.* 109, 605–612.  
608 <https://doi.org/10.1007/s00436-011-2292-9>  
609 Mayack, C., Naug, D., 2010. Parasitic infection leads to decline in hemolymph sugar levels in  
610 honeybee foragers. *J. Insect Physiol.* 56, 1572–1575.  
611 <https://doi.org/10.1016/j.jinsphys.2010.05.016>  
612 Mayack, C., Naug, D., 2009. Energetic stress in the honeybee *Apis mellifera* from *Nosema ceranae*  
613 infection. *J. Invertebr. Pathol.* 100, 185–188. <https://doi.org/10.1016/j.jip.2008.12.001>  
614 Medici, S.K., Sarlo, E.G., Porrini, M.P., Braunstein, M., Eguaras, M.J., 2012. Genetic variation and  
615 widespread dispersal of *Nosema ceranae* in *Apis mellifera* apiaries from Argentina. *Parasitol.*  
616 *Res.* 110, 859–864. <https://doi.org/10.1007/s00436-011-2566-2>  
617 Monnerie, S., Petera, M., Lyan, B., Gaudreau, P., Comte, B., Pujos-Guillot, E., 2019. Analytic  
618 Correlation Filtration: A New Tool to Reduce Analytical Complexity of Metabolomic Datasets.  
619 *Metabolites* 9. <https://doi.org/10.3390/metabo9110250>  
620 Naug, D., Gibbs, A., 2009. Behavioral changes mediated by hunger in honeybees infected with  
621 *Nosema ceranae*. *Apidologie* 40, 595–599. <https://doi.org/10.1051/apido/2009039>  
622 Nicholson, J.K., Foxall, P.J.D., Spraul, Manfred., Farrant, R.Duncan., Lindon, J.C., 1995. 750 MHz <sup>1</sup>H  
623 and <sup>1</sup>H-<sup>13</sup>C NMR Spectroscopy of Human Blood Plasma. *Anal. Chem.* 67, 793–811.  
624 <https://doi.org/10.1021/ac00101a004>  
625 Paris, L., El Alaoui, H., Delbac, F., Diogon, M., 2018. Effects of the gut parasite *Nosema ceranae* on  
626 honey bee physiology and behavior. *Curr. Opin. Insect Sci., Ecology •*  
627 *Parasites/Parasitoids/Biological control* 26, 149–154.  
628 <https://doi.org/10.1016/j.cois.2018.02.017>  
629 Pettis, J.S., vanEngelsdorp, D., Johnson, J., Dively, G., 2012. Pesticide exposure in honey bees results  
630 in increased levels of the gut pathogen *Nosema*. *Naturwissenschaften* 99, 153–158.  
631 <https://doi.org/10.1007/s00114-011-0881-1>  
632 Retschnig, G., Neumann, P., Williams, G.R., 2014. Thioclopid–*Nosema ceranae* interactions in honey  
633 bees: Host survivorship but not parasite reproduction is dependent on pesticide dose. *J.*  
634 *Invertebr. Pathol.* 118, 18–19. <https://doi.org/10.1016/j.jip.2014.02.008>

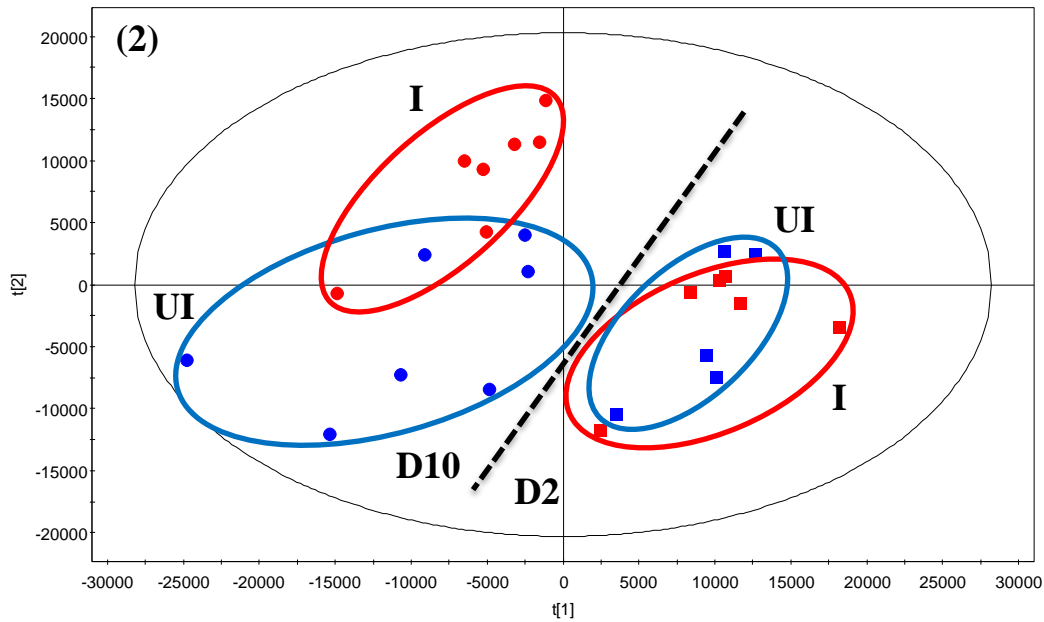
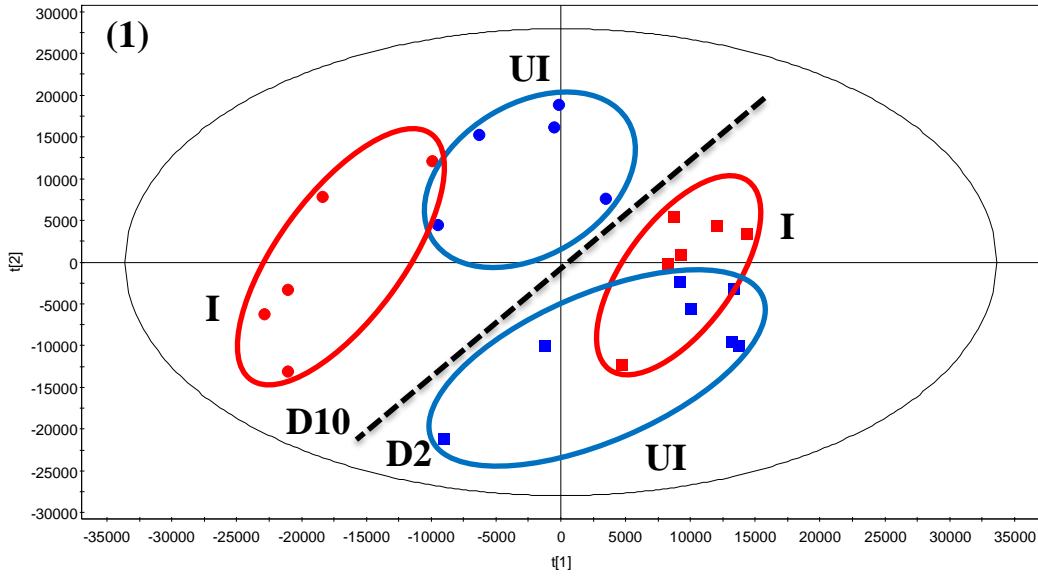
- 635 Simón-Manso, Y., Lowenthal, M.S., Kilpatrick, L.E., Sampson, M.L., Telu, K.H., Rudnick, P.A., Mallard,  
636 W.G., Bearden, D.W., Schock, T.B., Tchekhovskoi, D.V., Blonder, N., Yan, X., Liang, Y., Zheng,  
637 Y., Wallace, W.E., Neta, P., Phinney, K.W., Remaley, A.T., Stein, S.E., 2013. Metabolite  
638 Profiling of a NIST Standard Reference Material for Human Plasma (SRM 1950): GC-MS, LC-  
639 MS, NMR, and Clinical Laboratory Analyses, Libraries, and Web-Based Resources. *Anal.*  
640 *Chem.* 85, 11725–11731. <https://doi.org/10.1021/ac402503m>
- 641 The Metabolomics Standards Initiative (MSI) and Core Information for Metabolomics Reporting  
642 (CIMR) [WWW Document], n.d. URL [msi.html](http://msi.html) (accessed 3.10.20).
- 643 vanEngelsdorp, D., Evans, J.D., Saegerman, C., Mullin, C., Haubruge, E., Nguyen, B.K., Frazier, M.,  
644 Frazier, J., Cox-Foster, D., Chen, Y., Underwood, R., Tarpy, D.R., Pettis, J.S., 2009. Colony  
645 Collapse Disorder: A Descriptive Study. *PLOS ONE* 4, e6481.  
646 <https://doi.org/10.1371/journal.pone.0006481>
- 647 vanEngelsdorp, D., Meixner, M.D., 2010. A historical review of managed honey bee populations in  
648 Europe and the United States and the factors that may affect them. *J. Invertebr. Pathol.* 103,  
649 S80–S95. <https://doi.org/10.1016/j.jip.2009.06.011>
- 650 Vidau, C., Diogon, M., Aufauvre, J., Fontbonne, R., Viguès, B., Brunet, J.-L., Texier, C., Biron, D.G., Blot,  
651 N., El Alaoui, H., Belzunces, L.P., Delbac, F., 2011. Exposure to Sublethal Doses of Fipronil and  
652 Thiacloprid Highly Increases Mortality of Honeybees Previously Infected by *Nosema ceranae*.  
653 *PLoS ONE* 6. <https://doi.org/10.1371/journal.pone.0021550>
- 654 Wang, L., Meeus, I., Rombouts, C., Meulebroek, L.V., Vanhaecke, L., Smagghe, G., 2019.  
655 Metabolomics-based biomarker discovery for bee health monitoring: A proof of concept  
656 study concerning nutritional stress in *Bombus terrestris*. *Sci. Rep.* 9, 1–11.  
657 <https://doi.org/10.1038/s41598-019-47896-w>
- 658 Williams, G.R., Sampson, M.A., Shutler, D., Rogers, R.E.L., 2008. Does fumagillin control the recently  
659 detected invasive parasite *Nosema ceranae* in western honey bees (*Apis mellifera*)? *J.*  
660 *Invertebr. Pathol.* 99, 342–344. <https://doi.org/10.1016/j.jip.2008.04.005>
- 661 Willker, W., Engelmann, J., Brand, A., Liedfritz, D., 1996. Metabolite Identification in Cell Extracts and  
662 Culture Media by Proton-detected D-H, C-NMR Spectroscopy1. *J. Magn. Reson. Anal.* 21–32.
- 663 Wishart, D.S., Lewis, M.J., Morrissey, J.A., Flegel, M.D., Jeroncic, K., Xiong, Y., Cheng, D., Eisner, R.,  
664 Gautam, B., Tzur, D., Sawhney, S., Bamforth, F., Greiner, R., Li, L., 2008. The human  
665 cerebrospinal fluid metabolome. *J. Chromatogr. B Analyt. Technol. Biomed. Life. Sci.* 871,  
666 164–173. <https://doi.org/10.1016/j.jchromb.2008.05.001>
- 667 Wu, J.Y., Smart, M.D., Anelli, C.M., Sheppard, W.S., 2012. Honey bees (*Apis mellifera*) reared in brood  
668 combs containing high levels of pesticide residues exhibit increased susceptibility to *Nosema*  
669 (*Microsporidia*) infection. *J. Invertebr. Pathol.* 109, 326–329.  
670 <https://doi.org/10.1016/j.jip.2012.01.005>
- 671 Zhang, A., Sun, H., Wu, X., Wang, X., 2012. Urine metabolomics. *Clin. Chim. Acta* 414, 65–69.  
672 <https://doi.org/10.1016/j.cca.2012.08.016>
- 673 Zhang, X., Li, Q., Xu, Z., Dou, J., 2020. Mass spectrometry-based metabolomics in health and medical  
674 science: a systematic review. *RSC Adv.* 10, 3092–3104. <https://doi.org/10.1039/C9RA08985C>
- 675 Zhao, X., Fritsche, J., Wang, J., Chen, J., Rittig, K., Schmitt-Kopplin, P., Fritsche, A., Häring, H.-U.,  
676 Schleicher, E.D., Xu, G., Lehmann, R., 2010. Metabonomic fingerprints of fasting plasma and  
677 spot urine reveal human pre-diabetic metabolic traits. *Metabolomics* 6, 362–374.  
678 <https://doi.org/10.1007/s11306-010-0203-1>

## 679 680 **Web references**

- 681 « Human Metabolome Database ». <https://hmdb.ca/>.
- 682 « KEGG: Kyoto Encyclopedia of Genes and Genomes ». <https://www.genome.jp/kegg/>.
- 683 « MassBank | MSSJ MassBank Mass Spectral DataBase ». <http://www.massbank.jp/>.

684 « PRIME: Platform for RIKEN Metabolomics ».  
685 [http://prime.psc.riken.jp/?action=standard\\_index](http://prime.psc.riken.jp/?action=standard_index).

**Fig.1: PLS-DA on LC/MS profiles.**



R2X[1] = 0,209422

R2X[2] = 0,124118

Ellipse: Hotelling T2 (0,95)

SIMCA-P+ 12.0.1 - 2019-11-06 16:52:52 (UTC+1)

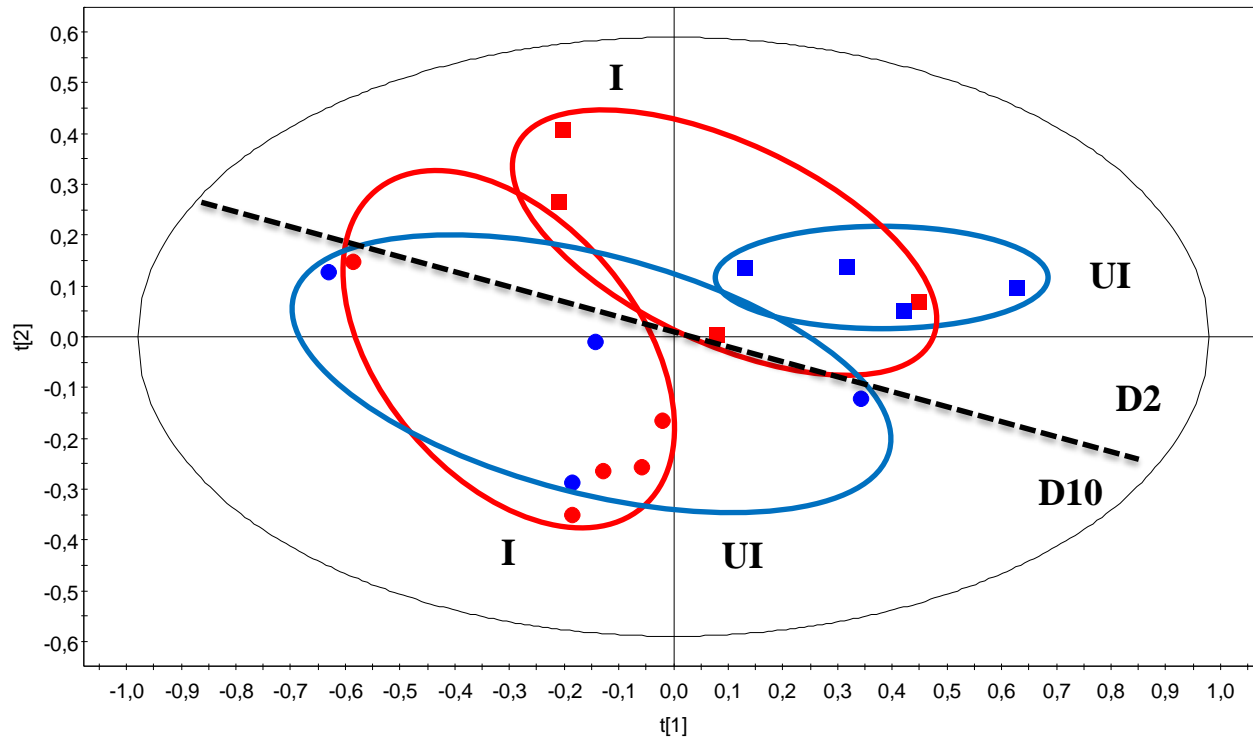


**Fig.2: PLS-DA on NMR data.**

